

# Simulations of liquid crystal hydrodynamics

Colin Denniston<sup>1</sup>, E. Orlandini<sup>2</sup>, and J.M. Yeomans<sup>1</sup>

<sup>1</sup> *Dept. of Physics, Theoretical Physics, University of Oxford, 1 Keble Road, Oxford OX1 3NP*

<sup>2</sup> *INFM-Dipartimento di Fisica, Università di Padova, 1-35131 Padova, Italy*

(May 5, 2021)

We present a lattice Boltzmann algorithm for liquid crystal hydrodynamics. The coupling between the tensor order parameter and the flow is treated consistently allowing investigation of a wide range of non-Newtonian flow behavior. We present results for the effect of hydrodynamics on defect coalescence; of the appearance of the log-rolling and kayaking states in Poiseuille flow; and for banding and coexistence of isotropic and nematic phases under shear.

83.70.Jr, 64.70.Md, 47.20.Ft, 83.10.Lk

There is growing interest in obtaining a fundamental physical understanding of the flow properties of liquid crystals, polymer melts, and droplet suspensions. The hydrodynamics of such complex fluids can be complicated and very different from that of simple liquids because of the coupling between the microscopic structure and the velocity fields imposed by the flow [1]. Examples include shear-thinning and thickening and non-equilibrium phase transitions such as banding under shear [2–4].

To understand the physics underlying such flow properties it is helpful to develop simulation techniques to probe the hydrodynamics of complex fluids. This has proved difficult because of the diverse length and time scales involved. Microscopic approaches, such as molecular dynamics, provide the most faithful representation of the microscopic physics. However they are not usually able to probe hydrodynamic time scales.

One attempt to surmount this problem has been the development of lattice Boltzmann simulations [5]. These solve the hydrodynamic equations of motion while inputting sufficient, albeit generic, molecular information to model the important physics of a given fluid. This is often done by imposing a Landau free energy functional, so the fluid evolves to a known thermodynamic equilibrium [6].

Most of the results thus far using lattice Boltzmann approaches have concentrated on the properties of binary fluid mixtures. Considerable progress has been made in understanding the effect of hydrodynamics on domain growth in 2- and 3-dimensions [7]. Investigations of flow have been more limited although there has been some work on binary solutions under oscillatory shear, on the flow of binary mixtures in porous media, and on amphiphilic fluids [5].

In this paper we describe a lattice Boltzmann algorithm for liquid crystal hydrodynamics. The aim is to investigate the wide range of physical phenomena which result because the director field couples to the flow. First we assess the effect of hydrodynamics on defect coalescence, a process important for phase ordering. This illustrates how the director configuration induces flow. We then examine the orientation of the director in Poiseuille flow. In addition to a steady state director configuration

for slower fluid velocities, the director can exhibit tumbling and chaotic orbits in rapid flows. Finally, we study the system under shear and demonstrate how the liquid crystal undergoes a non-equilibrium phase transition to a banded state where the bands are different phases co-existing at different strains but a unique stress [2,3].

We emphasize that almost all previous work has either ignored the flow, imposed a flow and worked out the director configuration ignoring back-flow effects, or coupled states of the director with states of flow using arguments based on the stability of interfaces. Here results are obtained self-consistently, by simulating the full hydrodynamics equations coupled to a description of the liquid crystal based on a tensor order parameter.

First we present the relevant equations of motion and the extensions of the lattice Boltzmann approach needed to solve them. A major difference from more simple fluids is that liquid crystals are described by a *tensor* order parameter  $\mathbf{Q}$  (related to the director  $\vec{n}$  by  $Q_{\alpha\beta} = \langle n_\alpha n_\beta - \frac{1}{3}\delta_{\alpha\beta} \rangle$ ). Their equilibrium properties can be described by the Landau-de Gennes free energy functional [8,9]

$$\mathcal{F} = k_B T \int d^3r \phi \left\{ \frac{1}{2} \left( 1 - \frac{\gamma}{3} \right) Q_{\alpha\beta} Q_{\beta\alpha} - \frac{\gamma}{3} Q_{\alpha\beta} Q_{\beta\zeta} Q_{\zeta\alpha} + \frac{\gamma}{4} (Q_{\alpha\beta} Q_{\beta\alpha})^2 + \frac{\kappa}{2} (\partial_\alpha Q_{\beta\zeta})^2 \right\} \quad (1)$$

where  $\phi$  is the liquid crystal concentration and  $T$  the temperature. The exact form of the coefficients of the bulk free energy terms is not important and for simplicity we write them in terms of a single parameter  $\gamma$  [10]. Similarly we restrict ourselves in the first instance to a single elastic constant  $\kappa$ .

The order parameter is not conserved. It evolves according to the convection-diffusion equation [3,9,11]

$$(\partial_t + \partial_\alpha u_\alpha) \mathbf{Q} = \mathbf{S}(\mathbf{W}, \mathbf{Q}) + (\Gamma/k_B T \phi) \mathbf{H}(\mathbf{Q}) \quad (2)$$

where  $\vec{u}$  is the bulk fluid velocity and  $\Gamma$  is a diffusion constant. Of the terms on the right-hand side of Eqn. (2)

$$\begin{aligned} \mathbf{S}(\mathbf{W}, \mathbf{Q}) = & (\lambda \mathbf{D} + \boldsymbol{\Omega})(\mathbf{Q} + \frac{1}{3}\mathbf{I}) + (\mathbf{Q} + \frac{1}{3}\mathbf{I})(\lambda \mathbf{D} - \boldsymbol{\Omega}) \\ & - 2\lambda(\mathbf{Q} + \frac{1}{3}\mathbf{I})\text{Tr}(\mathbf{Q}\mathbf{W}) \end{aligned} \quad (3)$$

accounts for the rotation of the nematic order parameter driven by the symmetric  $\mathbf{D}$ , and antisymmetric  $\mathbf{\Omega}$ , parts of the velocity gradients  $W_{\alpha\beta} = \partial_\beta u_\alpha$ . The parameter  $\lambda$  is related to the aspect ratio of the polymer molecule or alternatively can be viewed as a phenomenological parameter to correct for inaccuracies of quadratic closure [11]. The molecular field,

$$\mathbf{H} = - \left\{ \frac{\delta \mathcal{F}}{\delta \mathbf{Q}} - \frac{1}{3} \mathbf{I} \text{Tr} \frac{\delta \mathcal{F}}{\delta \mathbf{Q}} \right\} \quad (4)$$

describes the evolution to equilibrium in a way analogous to Model A.

The flow of the liquid crystal fluid obeys the continuity and Navier-Stokes equations

$$\partial_t \rho + \partial_\alpha \rho u_\alpha = 0, \quad (5)$$

$$\rho \partial_t u_\alpha + \rho u_\beta \partial_\beta u_\alpha = \partial_\beta \tau_{\alpha\beta} + \partial_\beta \sigma_{\alpha\beta} + 2\rho \tau_f / 3 (\partial_\beta (\delta_{\alpha\beta} + 3\partial_n \sigma_{\alpha\beta}) \partial_\zeta u_\zeta + \partial_\alpha u_\beta + \partial_\beta u_\alpha) \quad (6)$$

where

$$\sigma_{\alpha\beta} = -\rho T \delta_{\alpha\beta} - 3\mathbf{H}_{\alpha\beta} - \kappa (\partial_\alpha Q_{\zeta\delta} \partial_\beta Q_{\zeta\delta} - \partial_\lambda Q_{\zeta\delta} \partial_\lambda Q_{\zeta\delta} \delta_{\alpha\beta} / 2) \quad (7)$$

$$\tau_{\alpha\beta} = \mathbf{H}\mathbf{Q} - \mathbf{Q}\mathbf{H} \quad (8)$$

are the symmetric and antisymmetric contributions to the non-dissipative part of the stress tensor respectively.

A lattice Boltzmann scheme which reproduces equations (1) to (8) to second order can be defined in terms of two distribution functions  $f_i(\vec{x})$  and  $\mathbf{G}_i(\vec{x})$  where  $i$  labels lattice directions from site  $\vec{x}$ . Physical variables are related to the distribution functions by

$$\rho = \sum_i f_i, \quad \rho u_\alpha = \sum_i f_i e_{i\alpha}, \quad \mathbf{Q} = \sum_i \mathbf{G}_i. \quad (9)$$

The distribution functions evolve in a time step  $\Delta t$  according to

$$\begin{aligned} f_i(\vec{x} + \vec{e}_i \Delta t, t + \Delta t) - f_i(\vec{x}, t) &= \frac{\Delta t}{2} [\mathcal{C}_{f_i}(\vec{x}, t, \{f_i\}) + \\ &\quad \mathcal{C}_{f_i}(\vec{x} + \vec{e}_i \Delta t, t + \Delta t, \{f_i^*\})] \\ \mathbf{G}_i(\vec{x} + \vec{e}_i \Delta t, t + \Delta t) - \mathbf{G}_i(\vec{x}, t) &= \frac{\Delta t}{2} [\mathcal{C}_{\mathbf{G}_i}(\vec{x}, t, \{\mathbf{G}_i\}) + \\ &\quad \mathcal{C}_{\mathbf{G}_i}(\vec{x} + \vec{e}_i \Delta t, t + \Delta t, \{\mathbf{G}_i^*\})] \end{aligned} \quad (10)$$

where the collision operators are taken to have the form of a single relaxation time Boltzmann equation, together with a forcing term

$$\begin{aligned} \mathcal{C}_{f_i}(\vec{x}, t, \{f_i\}) &= \\ &\quad -\frac{1}{\tau_f} (f_i(\vec{x}, t) - f_i^0(\vec{x}, t, \{f_i\})) + p_i(\vec{x}, t, \{f_i\}), \\ \mathcal{C}_{\mathbf{G}_i}(\vec{x}, t, \{\mathbf{G}_i\}) &= \\ &\quad -\frac{1}{\tau_{\mathbf{G}}} (\mathbf{G}_i(\vec{x}, t) - \mathbf{G}_i^0(\vec{x}, t, \{\mathbf{G}_i\})) + h_i(\vec{x}, t, \{\mathbf{G}_i\}). \end{aligned} \quad (11)$$

$f_i^*$  and  $\mathbf{G}_i^*$  in equations (10) and (11) are first order approximations to  $f_i(\vec{x} + \vec{e}_i \Delta t, t + \Delta t)$  and  $\mathbf{G}_i(\vec{x} + \vec{e}_i \Delta t, t + \Delta t)$ . They are introduced to remove lattice viscosity terms to second order and they give improved stability.

The form of the equations of motion and thermodynamic equilibrium follow from the choice of the moments of the equilibrium distributions  $f_i^0$  and  $\mathbf{G}_i^0$  and the driving terms  $p_i$  and  $h_i$ .  $f_i^0$  is constrained by

$$\begin{aligned} \sum_i f_i^0 &= \rho, \quad \sum_i f_i^0 e_{i\alpha} = \rho u_\alpha, \\ \sum_i f_i^0 e_{i\alpha} e_{i\beta} &= -\sigma_{\alpha\beta} + \rho u_\alpha u_\beta \end{aligned} \quad (12)$$

where the zeroth and first moments are chosen to impose conservation of mass and momentum. The second moment of  $f^0$  controls the symmetric part of the stress tensor, whereas the moments of  $p_i$

$$\sum_i p_i = 0, \quad \sum_i p_i e_{i\alpha} = \partial_\beta \tau_{\alpha\beta}, \quad \sum_i p_i e_{i\alpha} e_{i\beta} = 0 \quad (13)$$

impose the antisymmetric part of the stress tensor.

For the equilibrium of the order parameter distribution we choose

$$\begin{aligned} \sum_i \mathbf{G}_i^0 &= \mathbf{Q}, \quad \sum_i \mathbf{G}_i^0 e_{i\alpha} = \mathbf{Q} u_\alpha, \\ \sum_i \mathbf{G}_i^0 e_{i\alpha} e_{i\beta} &= \mathbf{Q} u_\alpha u_\beta. \end{aligned} \quad (14)$$

This ensures that the fluid minimizes its free energy at equilibrium and that it is convected with the flow. Finally the evolution of the order parameter is most conveniently modeled by choosing

$$\begin{aligned} \sum_i h_i &= (D/k_B T \phi) \mathbf{H}(\mathbf{Q}) + \mathbf{S}(\mathbf{W}, \mathbf{Q}), \\ \sum_i h_i e_{i\alpha} &= (\sum_i h_i) u_\alpha. \end{aligned} \quad (15)$$

Conditions (12)–(15) can be satisfied by taking  $f_i^0$ ,  $\mathbf{G}_i^0$ ,  $h_i$ , and  $p_i$  as polynomial expansions in the velocity as is usual in lattice Boltzmann schemes [5]. A second order Chapman–Enskog expansion for the evolution equations (10) incorporating the conditions (12)–(15) leads to the equations of motion (2), (5), and (6).

The alternative Ericksen–Leslie–Parodi (ELP) equations of liquid crystal hydrodynamics are written in terms of the evolution of the director field  $\mathbf{n}$  [8] rather than the tensor order parameter  $\mathbf{Q}$ . We use the latter approach for two reasons. First, the motion of disclination lines (points in two dimensions) is explicitly included and it is particularly interesting to assess the effect of flow on this dynamics. Second, we are interested in examining phase transitions induced by shear and so need to describe both the isotropic and nematic phases. The ELP formalism

describes only the nematic phase at a fixed amplitude of order parameter. If we restrict the order parameter to be uniaxial with fixed amplitude, the  $\mathbf{Q}$  equations of motion can be reduced to the ELP equations. However, due to our choice of coefficients in, for example the free energy, we have specialized to three independent viscosity coefficients rather than the five in the ELP formalism. A lattice Boltzmann method for implementing the ELP equations is being studied elsewhere [12]

If Fig. 1 we show the flow fields induced when two disclinations of opposite sign mutually annihilate, a process important in phase separation. The director field induces a flow in the fluid in the form of vortices accompanying the disclinations [13]. Even after the defects have annihilated, they leave vortices behind in the fluid which then gradually decay away. The vortices induced in the fluid speed up the annihilation process, but do not change the  $t^{1/2}$  power law [14,15] for annihilation. This is because the vortex-vortex interaction is of the same form as the disclination-disclination interaction. However, in a system with many disclinations the interaction between annihilating pairs is likely to be much stronger when hydrodynamics is present as the fluid vortices left by the annihilation process are at a considerable distance from the annihilation site. We are currently examining the effect of hydrodynamics on the phase ordering.

A second example of the coupling between the director field and the flow is shown in Fig.2 where a Poiseuille flow is imposed on the liquid crystal with the director field pinned perpendicular to the flow direction at the boundaries. The director field couples to the shear component of the flow leading to a rich variety of possible dynamical states. For slow flows a static director field configuration is induced by the flow (Fig. 2(a)). We note that in order to match the director fields at the midpoint of the flow, the director orients *parallel* to the flow, not perpendicular as has been previously suggested [8], as this configuration has the lower elastic energy [16]. For faster, more rotational flows, or alternatively smaller  $\lambda$ , the “log rolling” state, where the director points perpendicular to the shear plane, has a lower viscosity and is more stable in the bulk. However, as the director is pinned in the shear plane at the boundary it must match the boundary configuration onto the log rolling state in the interior. The system is unable to do this with a steady state configuration and the director tumbles and kayaks (rotates in and out of the plane) in the interface region, as show in Figure 2(b). While the velocity profile remains nearly parabolic, as would be expected for Poiseuille flow in a simple fluid, the effective viscosity is strongly influenced by the state of the director.

Shear acts to orient the director field with respect to the flow and in this sense is analogous to a magnetic field in spin systems. As such, it can shift the transition from the isotropic (I) to nematic (N) phases [2,3,17]. The resulting non-equilibrium phase diagram in the shear-stress- $(1 - \gamma/3)$  plane (see Eqn. 1) consists of a line of first order phase transitions connecting to the

equilibrium transition at zero stress and terminating at a non-equilibrium critical point. This is illustrated in Figure 3(a) which shows the behavior of  $S_1$ , the largest eigenvalue of  $\mathbf{Q}$ , as a function of the shear stress. As  $\gamma$  is increased, the jump in the order parameter decreases and disappears at a non-equilibrium critical point.

In an experiment, or in our simulations, we do not have direct control over the shear stress (i.e. the total off diagonal stress, including elastic and viscous terms), but rather control the average strain rate (the relative velocity of the walls). The coexistence region is just a line on the stress-temperature phase diagram, but it corresponds to a finite region on a strain-temperature diagram. In fact the two different coexisting phases have a *different* strain rate. This phenomenon is known as shear banding and results in a plateau in the stress-strain curve shown in Figure 3(b). Once coexistence is reached, increasing the strain rate does not increase the stress, it just converts more of the system from the I to N phase. Once all the system is in the N phase, the stress again starts to increase. Our results are in agreement with those obtained in Ref. [2,3]. There an interface was imposed on a one-dimensional system and its stability was used to infer the state of the system. Here, shear banding is spontaneous and work is in progress to investigate the way in which the bands form.

In conclusion, we have derived and implemented a lattice Boltzmann algorithm for liquid crystal hydrodynamics. This opens the way to investigate a wide range of physical phenomena which result from the coupling between the director field and the flow, many of which have been examined only indirectly or with severe approximations in the past.

We thank G. Gonnella, C. Care and P. Olmsted for useful conversations. This work was funded in part by grants from the EPSRC.

- 
- [1] R.G. Larson, *Constitutive Equations for polymer melts and solutions*, Butterworths series in Chem. E., Butterworth (1988).
  - [2] P.D. Olmsted and P.M. Goldbart, Phys. Rev. A **46**, 4966 (1992).
  - [3] P.D. Olmsted and C.-Y. David Lu, Phys. Rev. E **56**, 55 (1997); *ibid*, **60**, 4397 (1999).
  - [4] M.E. Cates and S. T. Milner, Phys. Rev. Lett. **62**, 1856 (1989).
  - [5] S. Chen and G. D. Doolen, Annual Rev. Fluid Mech. **30**, 329 (1998).
  - [6] M.R. Swift, E. Orlandini, W.R. Osborn and J.M. Yeomans, Phys. Rev. E **54**, 5041 (1996).
  - [7] V.M. Kendon, J-C. Desplat, P. Bladon, and M.E. Cates, Phys. Rev. Lett. **83**, 576 (1999).

- [8] P.G. de Gennes and J. Prost, *The Physics of Liquid Crystals*, 2nd Ed., Clarendon Press, Oxford (1993).
- [9] M. Doi, J. Poly. Sci: Poly. Phys. **19**, 229 (1981); N. Kuzuu and M. Doi, J. Phys. Soc. Jap. **52**, 3486 (1983); M. Doi and S. F. Edwards, *The Theory of Polymer Dynamics*, Clarendon Press, Oxford, (1989).
- [10]  $\gamma$  is the Doi excluded volume parameter.
- [11] J.Feng, C.V. Chaubal and L.G. Leal, J. Rheol **42**, 1095 (1998).
- [12] C. Care, I. Halliday and K. Good, Private Communication, (1999).
- [13] This disagrees with the flow fields found in J.-i Fukuda, Eur. Phys. J. B **1**, 173 (1998). There, the flow appears to be nonexistent except for singularities (sources or sinks) at the site of the disclinations.
- [14] M. Zapotocky, P.M. Goldbart and N. Goldenfeld, Phys. Rev. E **51**, 1216 (1995).
- [15] C. Denniston, Phys. Rev. B **54**, 6272 (1996).
- [16] The director aligns with an angle  $\theta$  to the flow given by  $\cos 2\theta = 1/\xi$  where  $\xi$  is related to coefficients in equation (2). Since this implies  $\theta < \pi/4$  it will always cost less energy to have  $\theta = 0$  at the center rather than  $\theta = \pi/2$  as suggested in [8], pg 219.
- [17] H. See, M. Doi and R. Larson, J. Chem. Phys. **92**, 792 (1990).

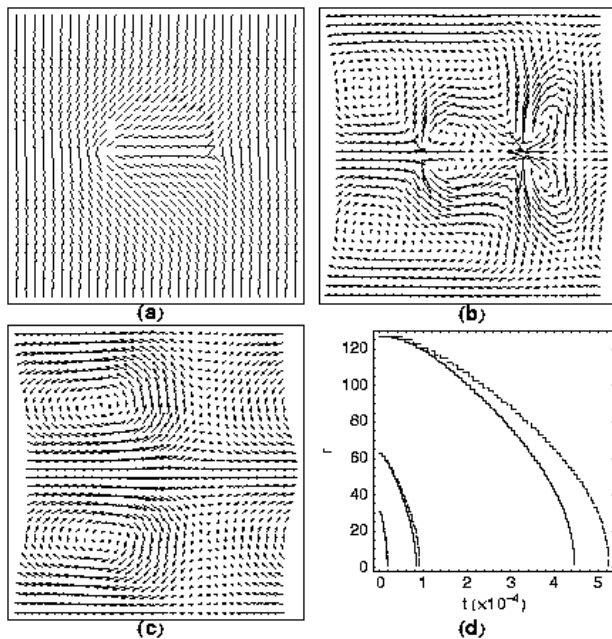


FIG. 1. (a) Director field for  $\pm 1/2$  disclinations moving towards annihilation. (b) Fluid velocity induced by the disclinations at the same time as the configuration shown in (a). (c) Vortices left in the fluid velocity field after the defects have annihilated. (d) Separation of the disclinations as a function of time for systems of sizes  $L = 64, 128$  and  $256$  (left to right) with (solid) and without (dashed) hydrodynamics. The disclinations start out at rest at a separation of  $L/2 - 1$ . Defects in systems with hydrodynamics annihilate faster.

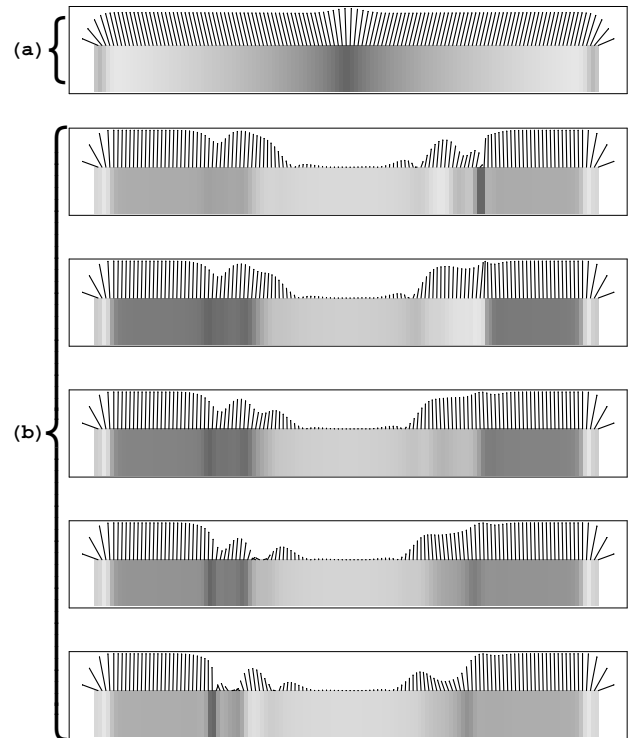


FIG. 2. Two different states in Poiseuille flow, where the lines represent the director orientation (eigenvector corresponding to largest eigenvalue of  $\mathbf{Q}$ ) projected down onto the  $xy$ -plane, and shading represents the amplitude of the order parameter (largest eigenvalue). Flow is from top to bottom, and the walls are at the left and right. At the walls, the director is aligned perpendicular to the boundary. (a) A stable configuration at low flow. (b) Snapshots of an oscillating configuration where the central region is in the "log-rolling state" (director perpendicular to the plane) and the boundary region consists of a transition from a configuration in the shear plane to a "tumbling" and "kayaking" region (director rotating in and out of the plane) interfacing to the central log-rolling state.

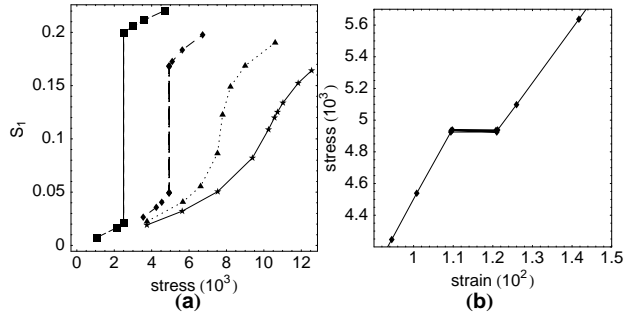


FIG. 3. (a) Amplitude of the order parameter  $S_1$  (largest eigenvalue of  $\mathbf{Q}$ ) as a function of the shear stress for  $\gamma = 2.65$  (squares), 2.6 (diamonds), 2.55 (triangles) and 2.5 (stars). The equilibrium transition occurs at  $\gamma \approx 2.7$ . (b) The stress-strain curve shows a discontinuity at the point where the shear stress induces a first-order, non-equilibrium phase transition from the weakly ordered paranematic I phase to the strongly ordered nematic N phase.